Hindawi Publishing Corporation
Journal of Powder Technology
Volume 2013, Article ID 946984, 5 pages
http://dx.doi.org/10.1155/2013/946984

Research Article

Improvement of the Contact Strength of Al_2O_3/SiC by a Combination of Shot Peening and Crack-Healing

Tomoya Oki, Hiroki Yamamoto, Toshio Osada, and Koji Takahashi

Faculty of Engineering, Yokohama National University, 79-5 Tokiwadai, Hodogaya-ku, Yokohama 240-8501, Japan

Correspondence should be addressed to Koji Takahashi; ktaka@ynu.ac.jp

Received 1 March 2013; Accepted 25 April 2013

Academic Editor: Kotoji Ando

Al_2O_3/SiC composite ceramics with high crack-healing ability were subjected to shot peening (SP) using zirconium oxide shots with several peening pressures and shot diameters. Specimens subjected to SP were heat-treated in air to heal the surface cracks induced by SP. The residual stress, the apparent fracture toughness, and the Weibull distribution of the contact strength were investigated, revealing that the combination of SP and crack-healing is effective for increasing the contact strength and decreasing the scatter of the contact strength of Al_2O_3/SiC.

1. Introduction

Shot peening (SP) is a procedure commonly utilized to increase the fatigue strength of metals. The compressive residual stress generated by SP prevents fatigue crack propagation. Recent studies have shown that the near-surface strength of ceramics can be improved by SP [1, 2]. Pfeiffer and Frey [1] reported that high compressive residual stress of up to more than 1 GPa could be introduced near the surface of alumina (Al_2O_3) and silicon nitride (Si_3N_4) substrates treated by SP using 650 μm tungsten carbide shots. Furthermore, Tanaka et al. [2] reported that compressive residual stress of up to 1.5 GPa was introduced near the surface of Si_3N_4 that was subjected to SP using 50 μm high-strength steel shots and 1100 μm tungsten carbide shots and that the compressive residual stress increased the apparent fracture toughness. Additionally, Moon et al. [3] reported that the residual stress which is introduced to Al_2O_3 by SP is attributed to microcracks and dislocation. Based on the results obtained in previous studies, SP treatment is a promising technique for increasing the strength of ceramics in the surface region. Strengthening the surface layer increases the contact strength of ceramic components such as bearings and cutting tools, for which higher contact strengths are desirable. However, unintentional introduction of cracks during the SP process may compromise the reliability of the ceramics components.

Certain structural ceramics exhibit crack-healing ability [4–7]. Thus, if crack-healing can be combined with SP, the surface strength and reliability of ceramics can be increased. Takahashi et al. [8, 9] investigated the effects of SP and crack-healing on the contact strength of an Si_3N_4/SiC composite. The Si_3N_4/SiC was subjected to SP using 300 μm zirconium oxide (ZrO_2) shots, and the contact strength of the Si_3N_4/SiC was reportedly increased by SP treatment [8]. It was also reported that the scatter of the contact strength in the SP specimens of the Si_3N_4/SiC could be improved by crack-healing in air at 1100°C for 5 h given that the surface cracks induced by SP were reduced by crack-healing. However, the combined effects of SP and crack-healing on the Al_2O_3/SiC composite have not yet been investigated.

In this study, the effects of shot peening and crack-healing on the residual stress, the apparent fracture toughness, and the Weibull distribution of contact strength are investigated for the Al_2O_3/SiC composite.

2. Test Procedure

2.1. Materials and Specimens. Silicon carbide reinforced alumina (Al_2O_3/SiC) was selected as a test material because it has excellent crack-healing ability [5, 6]. The Al_2O_3 powder (AKP-20, Sumitomo Chemical Co. Ltd., Japan) used in this study has an average particle size of 0.5 μm. The SiC powder (ultrafine grade, Ibiden Co. Ltd., Japan) used has a mean particle size of 0.27 μm. The samples were prepared using a mixture of Al_2O_3 with 15 vol.% SiC powder. Alcohol was then added to the solution, and the mixture was thoroughly homogenized by blending for 48 h. The mixture was placed in an evaporator to extract the solvent and then vacuum-treated to produce a dry powder. The mixture was subsequently hot-pressed at 1700°C and 35 MPa for 2 h under N_2 atmosphere. The hot-pressed plate was then cut into test specimens measuring 3 × 4 × 40 mm. The specimens were polished to a mirror finish on one face. These specimens are hereinafter referred to as "Smooth" specimens.

2.2. Crack-Healing and Shot Peening Conditions. The "Smooth" specimens were crack-healed in air at 1300°C for 1 h. These specimens are denoted "CH" (crack-healed) specimens. This crack-healed condition in which surface cracks of about 100 μm long can be healed fully was selected based on the results of a previous study [5, 6].

Shot peening (SP) was carried out on the "Smooth" specimens using a direct pressure peening system. Commercial zirconium oxide (ZrO_2) shots with a diameter of 180 μm were used. The Vickers hardness of the ZrO_2 shots was 1250 HV. The peening pressure selected was 0.1 MPa. The specimens were shot peened for 40 s. The peening coverage was 300%. The specimens subjected to SP are denoted as "SP" specimens. Following SP, the specimens were heat treated in air at 950°C for 100 h. The oxide film of 1-2 μm depth was then removed by polishing the specimens with diamond abrasives with a diameter of 1 μm. These specimens are denoted "SP + CH" specimens. This crack-healed condition was selected based on the results of a preliminary experiment [10]. Surface cracks introduced by SP can be healed while maintaining the compressive residual stress introduced by SP.

2.3. Residual Stress, Surface Roughness, and Apparent Fracture Toughness. The residual stresses on the surface were measured for Smooth, CH, SP, and SP + CH specimens via the X-ray diffraction method. The conditions for X-ray diffraction are shown in Table 1. The surface roughness was measured at five points on each specimen using a stylus-type surface roughness tester.

Smooth, CH, SP, and SP + CH specimens were prepared for measurement of the apparent fracture toughness (K_C) at the subsurface. The K_C was evaluated by the indentation fracture (IF) method, in which K_C can be estimated using the following equation in accordance with the Japan Industry Standards (JIS) [11]:

$$K_C = 0.026 E^{1/2} P^{1/2} \frac{a}{c^{3/2}}, \quad (1)$$

where E is Young's modulus, P is the indent load, a is half the diagonal length of the indentation, and c is half the surface crack length. Vickers indentations were introduced on the polished surface by applying an indent load of 49 N for 20 s. The Young's modulus of the material is 324 GPa, as determined by the strain measurements in the bending test.

2.4. Measurement of Contact Strength. Smooth specimens, CH specimens, SP specimens, and SP + CH specimens were subjected to contact strength measurement. The contact strength was measured using sphere indentation tests. Figure 1 shows the testing system. Indentations were made on the surfaces of the specimens using tungsten carbide (WC) spheres with a diameter of 4 mm. The sphere indentation tests were carried out at a crosshead speed of 0.2 kN/min using a universal testing machine. The ring crack initiation load (P_{max}) was determined using acoustic emission (AE). Loading was interrupted at the load at which crack initiation was detected by the AE system. The loads were then removed, and the indented surfaces were observed using optical microscopy to identify the point of crack initiation.

Figure 2 shows an example of a ring crack. The Weibull distributions of the crack initiation load were determined for each specimen. The distance between indentations was 4 mm, and thus the indentations were fully separated. In this study, the ring crack initiation loads (P_{max}) were statistically analyzed by a two-parameter Weibull function. In these analyses, the failure probability, F, was calculated using the median rank estimate. These results were plotted using the two-parameter Weibull function, expressed by the following equation:

$$F(P_{max}) = 1 - \exp\left\{-\left(\frac{P_{max}}{\beta}\right)^{\alpha}\right\}, \quad (2)$$

where P_{max} is the ring crack initiation load, α is the scale parameter, and β is the shape parameter. The scale parameter β describes the crack initiation load when $F(P_{max}) = 63.2\%$. The shape parameter α describes the width of the distribution of the crack initiation load.

3. Results and Discussion

3.1. Residual Stress. Compressive residual stress on the surface layer may reflect the volume expansion induced by microcrack initiation within crystallites [3]. Figure 3 shows the residual stress distributions for the SP (□) and SP + CH specimens (♦). The in-depth residual stress distribution was investigated after removing the surface layers by polishing the specimens with diamond abrasives of 9.0, 3.0, and 0.5 μm. The residual stress induced by polishing was also investigated by measuring the residual stress after polishing. A maximum compressive residual stress of 300 MPa was observed on the surface of the SP specimen. The compressive residual stress decreased in the depth direction. Compressive residual stress of up to approximately 10 μm was generated. The compressive residual stress decreased in the case of the SP + CH specimen, whereas this sample still exhibited a compressive residual stress of 200 MPa. Thus, the induction of compressive residual stress and crack-healing occurred simultaneously.

The lattice strain was relieved due to thermal expansion as a result of heat treatment. Crack-healing due to oxidation of SiC occurs above 800°C. The oxidation of SiC is accompanied by approximately 80% volume expansion of the condensing phase. The oxidation products fill the microcracks, which leads to volume expansion at the surface. Thus, the relaxation

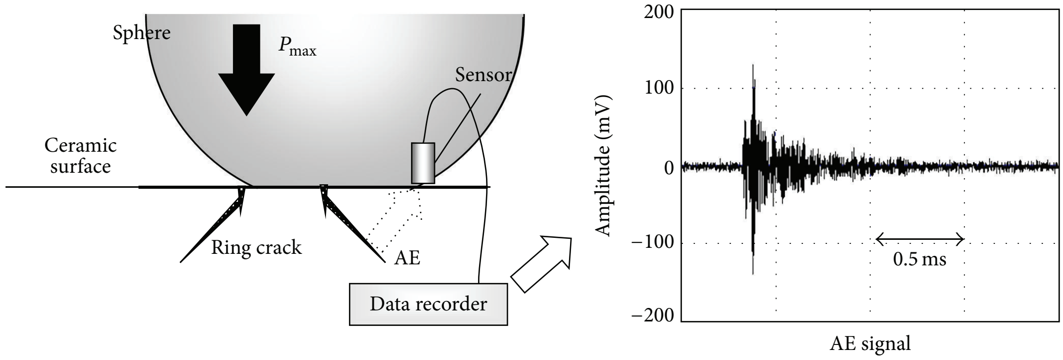

Figure 1: Schematic illustration of the sphere indentation test, ring cracks on the surface, and AE signal.

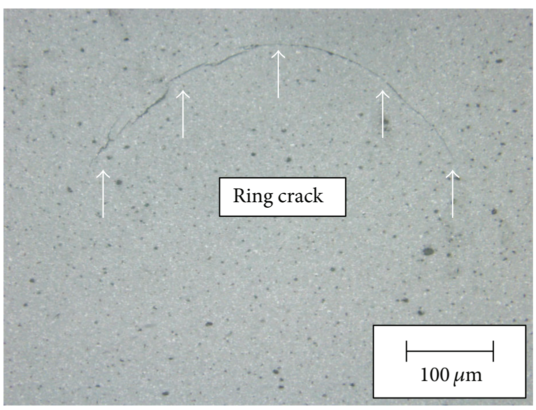

Figure 2: A ring crack after the sphere indentation test.

Table 1: Conditions for X-ray diffraction.

Characteristic X-ray	Cr-Kα
X-ray tube	Cu
Diffraction plane	Al_2O_3 (146)
Diffraction angle (deg)	136.11
Tube voltage (kV)	40
Tube current (mA)	30

Table 2: Surface roughness of each test specimen.

Specimens	Maximum height roughness R_z (μm)
Smooth	0.445
SP	0.498
SP + CH (950°C for 100 h)	0.471
SP + CH (950°C for 100 h) Nonpolishing	0.530
CH (1300°C for 1 h)	0.554

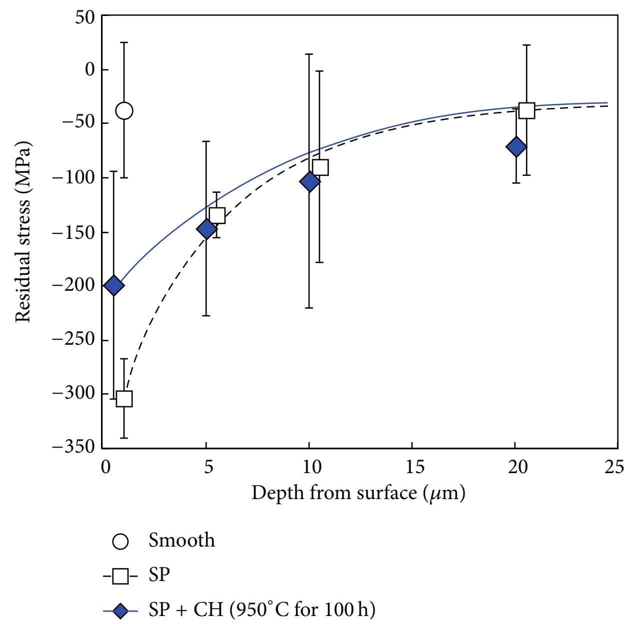

Figure 3: Relationship between residual stress and depth from the surface.

of compressive residual stress was not pronounced after crack-healing [8, 9].

3.2. Surface Roughness. Table 2 shows the average value of the surface roughness for each specimen. It can be seen that the surface roughness increased after SP treatment. However, the extent of this increase was quite small. Thus, it can be deduced that SP treatment can be effectively applied to ceramic components. The surface roughness increased after heat treatment due to oxidation of the surface layer by heat treatment in air. The surface roughness values of the SP + CH specimens were comparable to those obtained for the Smooth specimens given that the oxide film was removed by polishing. However, it is estimated that contact strength is not affected by surface roughness because the variation of surface roughness is small.

3.3. Apparent Fracture Toughness. Figure 4 shows the apparent fracture toughness (K_C) at the sub-surface measured by the IF method. The K_C increased by 96% in the case of the SP specimens in contrast with the K_C for the Smooth specimens. Subsequent to heat treatment, the K_C of the SP specimens decreased. Nevertheless, the K_C of the SP specimen after heat treatment was 50% higher than that of the Smooth specimen.

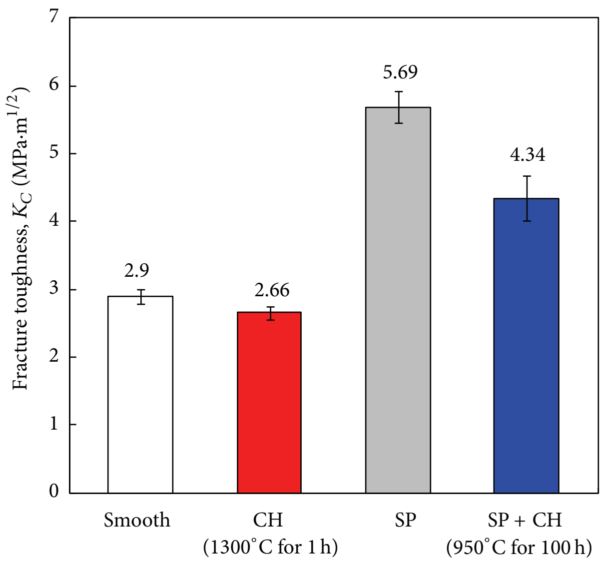

Figure 4: Apparent fracture resistance of each surface-treated specimen.

Table 3: Shape parameter α and scale parameter β of contact strength.

Specimens	Shape parameter α	Scale parameter β (kN)
Smooth	5.00	0.50
SP	2.76	0.96
SP + CH (950°C for 100 h)	5.18	0.92
CH (1300°C for 1 h)	6.22	0.60

Thus, SP in combination with crack-healing can improve K_C while healing the surface crack.

3.4. Contact Strength. Figure 5 shows the effects of shot peening and crack-healing on the Weibull distribution of the P_{max}. The shape parameter and scale parameter of the P_{max} obtained from the Weibull distribution are summarized in Table 3.

3.4.1. Effects of Crack-Healing. Good linearity of the Weibull distribution of P_{max} was achieved for the Smooth (○) and CH specimens (•). The scale parameter of CH specimens increased by 20% in contrast with that of the Smooth specimens. Thus, the value of P_{max} of the CH specimens increased in contrast with that of the Smooth specimens. The shape parameter of CH specimens increased by 24.4% in contrast with that of the Smooth specimens. Thus, the scatter of the P_{max} decreased in the case of the CH specimens in contrast with that of the Smooth specimens. This is due to the healing of the minute surface cracks introduced by the machining of the Smooth specimens.

3.4.2. Effects of Shot Peening. The scale parameter of SP specimens increased by 84%. Thus, the mean value P_{max} of the SP specimens increased in contrast with that of the Smooth specimens. However, the shape parameter of SP specimens decreased by 44.8% in contrast with that of the Smooth specimens. Moreover, the Weibull distribution of P_{max} for the SP specimens (□) was not characterized by good linearity in contrast with that of the Smooth specimens (○). Possible reasons for the nonlinearity of the Weibull distribution of the SP specimens are considered as follows.

In the lower fracture probability region, the P_{max} values of the SP specimens were smaller than those of the Smooth specimens given that the surface cracks induced by SP were present near the sphere indentation site. The P_{max} depends on the size and distribution of the cracks induced by SP. When a large crack is present near the sphere indentation site, the P_{max} tended to decline.

In the higher fracture probability regions, the P_{max} values of the SP specimens were larger than those of the Smooth specimens. It was presumed that the size of the surface cracks near the sphere indentation site was small. Thus, the crack initiation load increased because of the effect of the compressive residual stress.

3.4.3. Effects of Combination of Shot Peening and Crack-Healing. The scale parameter of SP + CH specimens increased by 84% and 53% in contrast with that of the Smooth and CH specimens, respectively. Thus, it is clear that the SP + CH specimens exhibited higher P_{max} than the Smooth and CH specimens. The shape parameter of SP + CH specimens increased by 87.8% in contrast with that of the SP specimens. Thus, it is also clear that the P_{max} values of the SP + CH specimens were characterized by a smaller scatter than those of the SP specimens. Thus, SP in combination with crack-healing is a useful technique for improving the contact strength of ceramics.

In the lower fracture probability region, the P_{max} values of the SP + CH specimens (⧫) were higher than those of the SP specimens (□), which is attributed to the healing of the cracks induced by SP for the former samples.

In the higher fracture probability region, the P_{max} values of the SP + CH specimens were larger than those of the Smooth (○) and CH specimens (•) given that the minute surface cracks introduced during machining of the Smooth specimens were healed, and a compressive residual stress of 200 MPa remained on the specimen surface. However, the P_{max} of the SP + CH specimens was slightly lower than that of the SP specimens given that the compressive residual stress decreased due to the heat treatment, as discussed in Section 3.1.

4. Conclusions

The effects of shot peening (SP) and crack-healing on the residual stress, the apparent fracture toughness, and the Weibull distribution of contact strength were investigated using an Al_2O_3/SiC composite. The results are summarized as follows.

(1) Compressive residual stresses of about 300 MPa were observed at the surface of the SP specimens.

(2) The apparent fracture toughness (K_C) at the sub-surface of the SP specimens increased by 96% for

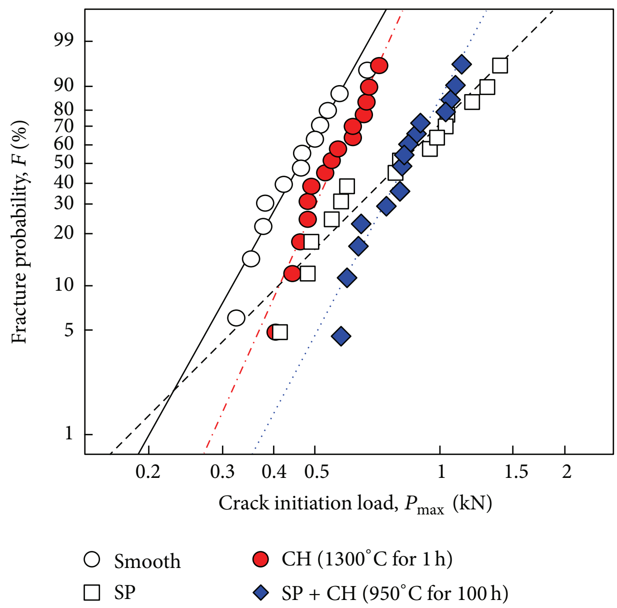

FIGURE 5: Effects of shot peening and crack-healing on the Weibull distribution of crack initiation load.

the SP specimen in comparison with the K_C for the Smooth specimens.

(3) The compressive residual stress and the K_C of the SP + CH specimens decreased in contrast with the SP specimens. However, the K_C value of the SP + CH specimens was 50% higher than that of the Smooth specimen. Thus, it could be deduced that the induction of compressive residual stress and crack-healing occurred simultaneously.

(4) The SP specimens exhibited the highest crack initiation load (P_{max}) of the evaluated specimens. However, the scatter of the P_{max} values was larger in the case of the SP specimens than that of the values of the other specimens because cracks induced during the SP process were present near the specimen surface.

(5) The scatter of the P_{max} values of the SP specimens could be improved by crack-healing in air at 950°C for 100 h given that the surface cracks induced by SP were effectively healed.

(6) On the basis of the results discussed in points (1) to (5), it can be concluded that SP in combination with crack-healing is a useful technique for improving the contact strength of ceramics.

Acknowledgment

The authors thank Dr. Shinji Saito from NHK Spring co. ltd. for his cooperation on the experiments.

References

[1] W. Pfeiffer and T. Frey, "Strengthening of ceramics by shot peening," *Journal of the European Ceramic Society*, vol. 26, no. 13, pp. 2639–2645, 2006.

[2] K. Tanaka, Y. Akiniwa, and Y. Morishita, "Residual stress distribution in the sub-surface region of shot-peened ceramics," *Nihon Kikai Gakkai Ronbunshu, A Hen/Transactions of the Japan Society of Mechanical Engineers, Part A*, vol. 71, no. 12, pp. 1714–1721, 2005.

[3] W. J. Moon, T. Ito, S. Uchimura, and H. Saka, "Toughening of ceramics by dislocation sub-boundaries," *Materials Science and Engineering A*, vol. 387–389, no. 1-2, pp. 837–839, 2004.

[4] S. R. Choi and V. Tikare, "Crack healing behavior of hot pressed silicon nitride due to oxidation," *Scripta Metallurgica et Materiala*, vol. 26, no. 8, pp. 1263–1268, 1992.

[5] M. C. Chu, S. Sato, Y. Kobayashi, and K. Ando, "Damage healing and strengthening behaviour in intelligent mullite/SiC ceramics," *Fatigue and Fracture of Engineering Materials and Structures*, vol. 18, no. 9, pp. 1019–1029, 1995.

[6] K. Ando, B. S. Kim, M. C. Chu, S. Saito, and K. Takahashi, "Crack-healing and mechanical behaviour of Al_2O_3/SiC composites at elevated temperature," *Fatigue and Fracture of Engineering Materials and Structures*, vol. 27, no. 7, pp. 533–541, 2004.

[7] K. Takahashi, M. Yokouchi, S. K. Lee, and K. Ando, "Crack-healing behavior of Al2O3 toughened by SiC whiskers," *Journal of the American Ceramic Society*, vol. 86, no. 12, pp. 2143–2147, 2003.

[8] K. Takahashi, Y. Nishio, Y. Kimura, and K. Ando, "Improvement of strength and reliability of ceramics by shot peening and crack healing," *Journal of the European Ceramic Society*, vol. 30, no. 15, pp. 3047–3052, 2010.

[9] K. Takahashi and Y. Nishio, "Improvement of the contact strength of Si_3N_4/SiC by a combination of shot peening and crack-healing," *Journal of Solid Mechanics and Materials Engineering*, vol. 3, no. 1, pp. 41–52, 2012.

[10] T. Oki, *Master Thesis in Yokohama National University*, 2013.

[11] R1607, *Testing Method for Fracture Toughness of Fine Ceramics*, Japan Standards Association, 1995.

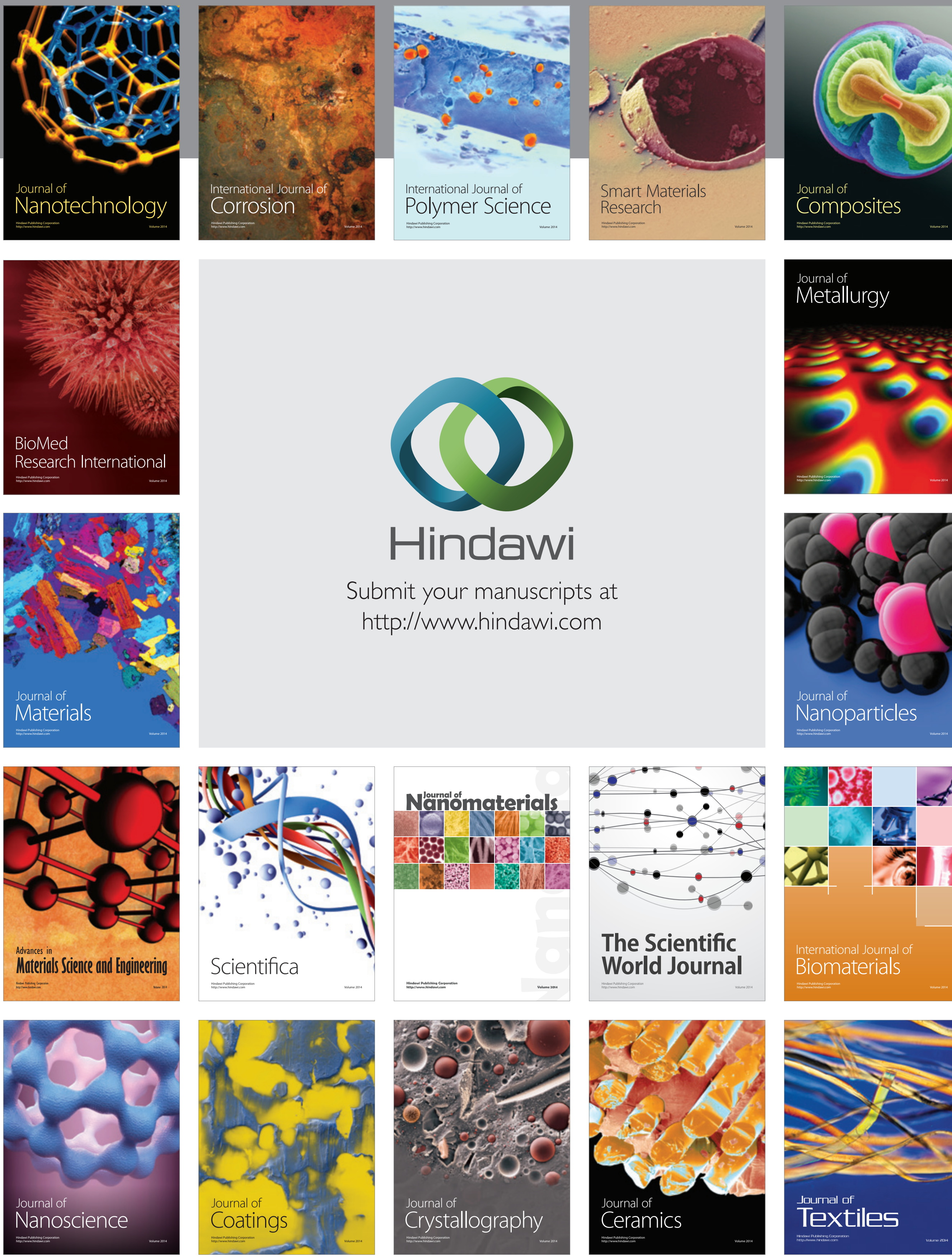
Journal of Nanotechnology
International Journal of Corrosion
International Journal of Polymer Science
Smart Materials Research
Journal of Composites
BioMed Research International
Hindawi
Submit your manuscripts at
http://www.hindawi.com
Journal of Metallurgy
Journal of Materials
Journal of Nanoparticles
Advances in Materials Science and Engineering
Scientifica
Journal of Nanomaterials
The Scientific World Journal
International Journal of Biomaterials
Journal of Nanoscience
Journal of Coatings
Journal of Crystallography
Journal of Ceramics
Journal of Textiles